symmetry

MDPI

Article

Response of Shock Isolators with Piecewise Linear Asymmetric Damping

Ana-Maria Mitu [1,*], Ovidiu Solomon [1,2,*], Marius Giuclea [1,2] and Tudor Sireteanu [1]

[1] Institute of Solid Mechanics of the Romanian Academy, 15 Constantin Mille, 010141 Bucharest, Romania; marius.giuclea@csie.ase.ro (M.G.); tudor.sireteanu@imsar.ro (T.S.)
[2] Department of Applied Mathematics, Bucharest University of Economic Studies, 6 Romana Square, 010374 Bucharest, Romania
* Correspondence: anamaria.mitu@imsar.ro (A.-M.M.); ovidiu.solomon@csie.ase.ro (O.S.)

Abstract: The output of a single-degree-of-freedom (SDOF) piecewise linear system with asymmetric damping and linear stiffness excited by Dirac impulse excitation is studied. Analytical solutions of the response for piecewise linear systems are obtained by replacing the equation of motion with Dirac excitation by a homogeneous differential system with zero initial displacement and a given initial velocity. A significant improvement of the response consisting in a substantial reduction in the after-shock vibrations was obtained. The obtained results are applied to the damping optimization of a shock isolation system for forging hammers.

Keywords: shock isolation system; asymmetric damping; forging hammer

1. Introduction

The study of reducing the effects of shocks on mechanical structures aims to minimize the transmitted forces through a shock isolation system and maintain absolute displacements within the admissible limits. The effects of nonlinear stiffness on a shock isolator's performance were studied in [1]. An optimal shock isolation system with quadratic damping and linear stiffness showed better performance than conventional isolators [2]. A methodology to derive the optimal parameters for shock isolated systems for high acceleration levels arising from explosions was presented in [3]. The influence of a damper on the dynamic responses of a vehicle are investigated analytically under bump and pothole excitations [4]. A method of obtaining the closed-form displacement response of free undamped vibrations and the steady state of forced damped vibrations of systems with piecewise linear springs is presented in [5]. An effective and low-cost method to assess the condition of vehicles' shock absorbers, based on the measurement of vertical accelerations on sprung and unsprung masses for a shock input, was proposed in [6]. The effects of shock absorber asymmetry on the vibration responses of a seat-occupant system under impact conditions are explored in [7]. Another type of device widely used for shock vibrations is represented by wire rope isolators, characterized by symmetric responses (hysteresis loops) when they deform transversally, as show in [8], and asymmetric responses when they are loaded along their axial direction, as illustrated in [9].

For linear shock isolation systems, an optimal relative damping value was determined so as to minimize the acceleration output for any stiffness [10–12]. In this case, the control of the maximum displacement is achieved through a convenient choice of system stiffness, so that the maximum acceleration does not exceed the admissible limit. For an imposed maximum admissible displacement, the optimal value of the relative damping that minimizes the transmitted acceleration was determined in [10–12]. Therefore, the maximum acceleration is controlled by the stiffness of the system, which is determined by the maximum imposed displacement.

check for updates

Citation: Mitu, A.-M.; Solomon, O.; Giuclea, M.; Sireteanu, T. Response of Shock Isolators with Piecewise Linear Asymmetric Damping. *Symmetry* **2023**, *15*, 1921. https://doi.org/10.3390/sym15101921

Academic Editor: Antonio Palacios

Received: 11 September 2023
Revised: 2 October 2023
Accepted: 13 October 2023
Published: 16 October 2023

In the case of piecewise linear (PWL) systems, the maximum acceleration and the maximum displacement of the system's response to shock input are the same as those obtained in the case of linear systems. The advantage of PWL systems lies in the fact that the after-shock oscillations can be substantially reduced by the asymmetry of the damping characteristic without affecting the optimal values of acceleration and displacement obtained in the case of linear systems.

In most cases, shock isolation systems have constant stiffness and different compression and extension values of their dissipative characteristic. These systems can be practically made more simply than those with different values of compression and expansion stiffness. The beneficial effect of asymmetric damping is studied in the present paper for a shock isolation system with a Dirac input. This approach allows us to obtain analytical solutions for the response of PWL systems in the first sequence by replacing the equation of motion with Dirac excitation (with zero initial conditions) with a homogeneous differential system with zero initial displacement and given initial velocity [13].

The response of hammer foundations to different pulse loadings is investigated in [14]. The effects of pulse shape and pulse duration on the dynamic response of a one-mass hammer-foundation system were studied in [15]. A system dynamics model for an isolated foundation and solution technique for obtaining the system response under impact loads is introduced in [16]. The effects of the shape and duration of a pulse load on the dynamic response of a hammer-foundation forging system were assessed in [17]. The mechanical vibrations of a specific forging hammer were investigated in order to understand the influence of different control parameters on forging efficiency [18]. A linearization method for the hysteretic dissipative characteristics of devices used for reducing shocks generated by forging hammers is presented in [19].

In this paper, the output of an SDOF piecewise linear system with asymmetric damping and linear stiffness, excited by Dirac impulse excitation, is studied. The obtained results are applied to the damping optimization of a shock isolation system for forging hammers. A significant improvement in the response consisting in a substantial reduction in the after-shock vibrations was obtained. This improvement leads to the possibility of shortening the action time of the forge hammer between two blows.

This paper is organized as follows: Section 2 includes some results regarding the optimization of linear systems with respect to the minimum absolute value of the acceleration response. The optimization of the acceleration response for an imposed maximum value of displacement is presented in Section 3. Section 4 contains the response of the PWL system to the shock input, and the optimization of the PWL system for shock input is illustrated in Section 5. An application of shock isolation for forging hammers is described in Section 6. The last section presents our conclusions.

2. Optimization of Linear Systems with Respect to the Minimum Acceleration Response

Consider the linear system with Dirac impulse excitation:

$$\begin{array}{l} \ddot{x} + 2\zeta\omega\dot{x} + \omega^2 x = -V_0\delta(t),\ V_0 > 0 \\ x(0) = 0,\ \dot{x}(0) = 0 \end{array}. \tag{1}$$

System (1) has the same solution as the linear system with nonzero initial velocity.

$$\begin{array}{l} \ddot{x} + 2\zeta\omega\dot{x} + \omega^2 x = 0 \\ x(0) = 0,\ \dot{x}(0) = V_0 \end{array}. \tag{2}$$

The solution of system (2) is given by [13]:

$$x(t,\zeta,\omega) = \frac{V_0}{\omega\sqrt{1-\zeta^2}} e^{-\zeta\omega t} \sin\left[\omega\sqrt{1-\zeta^2}t\right],\ t \geq 0 \tag{3}$$

The maximum absolute values $x_{m1}(\zeta,\omega)$ and $x_{m2}(\zeta,\omega)$ of the first and second peaks of displacement $x(t,\zeta,\omega)$ are obtained for

$$t_{d1}(\zeta,\omega)=\frac{\theta+\frac{\pi}{2}}{\omega\sqrt{1-\zeta^2}},t_{d2}(\zeta,\omega)=\frac{\theta+\frac{3\pi}{2}}{\omega\sqrt{1-\zeta^2}} \tag{4}$$

where

$$\theta=\arctan\left(\frac{-\zeta}{\sqrt{1-\zeta^2}}\right) \tag{5}$$

Introducing (4) into (3), the ratio $r_d(\zeta)$ of absolute values of the second and first peaks of displacement $x(t,\zeta,\omega)$ are given by

$$r_d(\zeta)=\frac{x_{m2}(\zeta,\omega)}{x_{m1}(\zeta,\omega)}=e^{-\frac{\zeta\pi}{\sqrt{1-\zeta^2}}}. \tag{6}$$

The ratio $r_d(\zeta)$ is plotted in Figure 1.

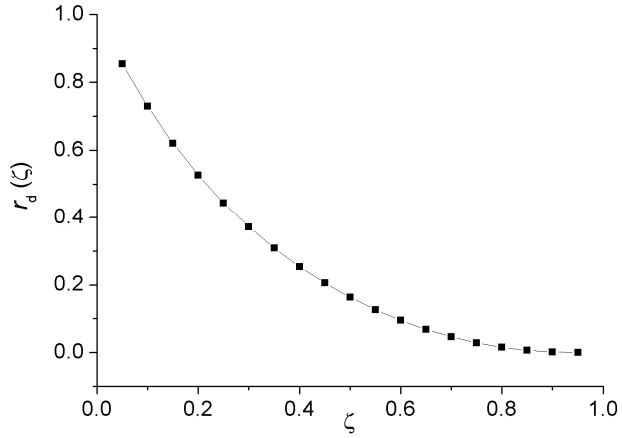

Figure 1. The ratio of absolute values of the second and first peaks of displacement.

The velocity and acceleration of the sprung mass are

$$\begin{aligned}\dot{x}(t,\zeta,\omega)&=\frac{V_0}{\sqrt{1-\zeta^2}}e^{-\zeta\omega t}\cos\left(\omega\sqrt{1-\zeta^2}t-\theta\right)\\ \ddot{x}(t,\zeta,\omega)&=-\omega\frac{V_0}{\sqrt{1-\zeta^2}}e^{-\zeta\omega t}\sin\left(\omega\sqrt{1-\zeta^2}t-2\theta\right)\end{aligned} \tag{7}$$

The time moments at which the maximum absolute values of velocity and acceleration are reached, are given by

$$\begin{aligned}t_v(\zeta,\omega)&=\frac{2\theta+\pi}{\omega\sqrt{1-\zeta^2}}\\ t_a(\zeta,\omega)&=\frac{3\theta+\frac{\pi}{2}}{\omega\sqrt{1-\zeta^2}}\end{aligned} \tag{8}$$

As a consequence, the maximum absolute value of velocity is

$$\dot{x}_m(\zeta,\omega)=V_0e^{-\zeta\omega t_v}=V_0e^{-\zeta\frac{2\theta+\pi}{\sqrt{1-\zeta^2}}}, \tag{9}$$

and the maximum absolute value of acceleration is given by

$$\dot{x}_m(\zeta,\omega)=V_0e^{-\zeta\omega t_v}=V_0e^{-\zeta\frac{2\theta+\pi}{\sqrt{1-\zeta^2}}}, \tag{10}$$

The value of ζ_{opt} that minimizes the maximum absolute value of acceleration is obtained from the equation

$$\frac{d\ddot{x}_m(\zeta,\omega)}{d\zeta}=0. \tag{11}$$

Solving this nonlinear Equation (11) yields $\zeta_{opt}\cong 0.265$, for any value of ω [10–12]. Figure 2 shows the variation in the maximum acceleration $\ddot{x}_m(\zeta,\omega)$ of the linear system (2) in relation to the damping ratio ζ for $\omega=2\pi$ rad/s.

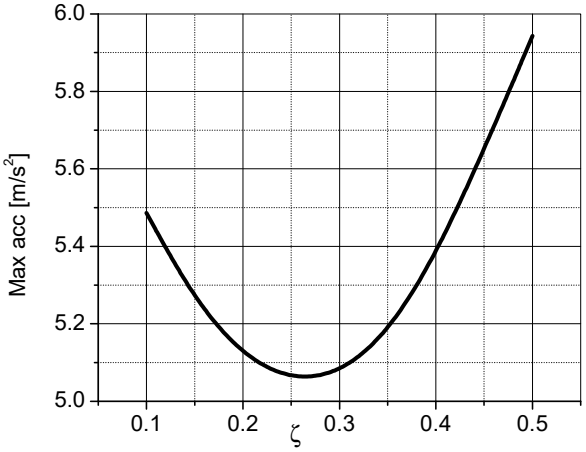

Figure 2. Variation in maximum acceleration versus damping ratio.

This result is important from a practical point of view because it shows that the minimum force transmitted due to the shock for any stiffness value of the isolation system is obtained for the same value of the relative damping coefficient. This optimization criterion could be contradictory to the limitation of maximum travel, admissible by the geometry of the vibration isolation system.

3. The Optimization of the Acceleration Response for an Imposed Maximum Displacement

The optimization of the acceleration response $\ddot{x}_m$ for an imposed maximum displacement $\overline{x}_m$, required by the maximum admissible stroke of the shock isolation device, is based on relations (6) and (10):

$$\begin{cases} \frac{V_0}{\omega} e^{-\zeta \frac{\arctan\left(\frac{-\zeta}{\sqrt{1-\zeta^2}}\right)+\frac{\pi}{2}}{\sqrt{1-\zeta^2}}} = \overline{x}_m \\ \ddot{x}_m(\zeta, \omega) = \omega V_0 e^{-\zeta \frac{3\arctan\left(\frac{-\zeta}{\sqrt{1-\zeta^2}}\right)+\frac{\pi}{2}}{\sqrt{1-\zeta^2}}} = \min \end{cases}. \tag{12}$$

From the first equation of system (12), we obtain

$$\omega = \frac{V_0}{\overline{x}_m} e^{-\zeta \frac{\arctan\left(\frac{-\zeta}{\sqrt{1-\zeta^2}}\right)+\frac{\pi}{2}}{\sqrt{1-\zeta^2}}}. \tag{13}$$

By introducing (13) into the second equation of (12), we achieve

$$\ddot{x}_m(\zeta) = \frac{V_0^2}{\overline{x}_m} e^{-\zeta \frac{4\arctan\left(\frac{-\zeta}{\sqrt{1-\zeta^2}}\right)+\pi}{\sqrt{1-\zeta^2}}}. \tag{14}$$

From $\frac{d\ddot{x}_m(\zeta)}{d\zeta} = 0$, one can derive

$$4\zeta\sqrt{1-\zeta^2} + 4\arctan\frac{\zeta}{\sqrt{1-\zeta^2}} - \pi = 0. \tag{15}$$

which has a unique solution $\zeta_m \cong 0.4$ at the interval $(0, 1)$. This result shows that for this value of the relative damping coefficient, the force transmitted due to the shock, for any imposed value of the maximum displacement isolation system, is minimal.

Introducing this value into (13) and (14), yields

$$\omega_m \cong 0.6\frac{V_0}{\overline{x}_m} \tag{16a}$$

$$\ddot{x}_{\mathrm{m}} \cong 0.52\frac{V_0^2}{\overline{x}_{\mathrm{m}}}. \tag{16b}$$

The relationship between the optimal value of maximum acceleration $\ddot{x}_{\mathrm{m}}(\zeta_{\mathrm{m}})$ obtained for an imposed maximum displacement $\overline{x}_{\mathrm{m}}$ and initial velocity V_0 is $\ddot{x}_{\mathrm{m}}(\zeta_{\mathrm{m}})\overline{x}_{\mathrm{m}} \geq \frac{V_0^2}{2}$. As one can see, this relation, which is used to specify the performance of the shock isolator, is fulfilled for any values of $\overline{x}_{\mathrm{m}}$ and V_0 in the case of Dirac impulse excitation [2].

From the equation $\dddot{x}(t, \zeta_{\mathrm{m}}, \omega_{\mathrm{m}}) = 0$, the second peak value of acceleration is given by

$$\ddot{x}_{\mathrm{m2}}^{\mathrm{LIN}} = \mathrm{V}_0\omega_{\mathrm{m}} \exp\left[-\left(\frac{\zeta_{\mathrm{m}}\arccos\left(2\zeta_{\mathrm{m}}^2-1\right)}{\sqrt{1-\zeta_{\mathrm{m}}^2}} + \frac{\zeta_{\mathrm{m}}\arctan\left(\frac{\sqrt{1-\zeta_{\mathrm{m}}^2}}{\zeta_{\mathrm{m}}}\right)}{\sqrt{1-\zeta_{\mathrm{m}}^2}}\right)\right] \cong 0.13\frac{V_0^2}{\overline{x}_{\mathrm{m}}}. \tag{17}$$

Using (16) and (17), the ratio of the maximum values of the second peak $\ddot{x}_{\mathrm{m2}}$ and first peak $\ddot{x}_{\mathrm{m1}} = \ddot{x}_{\mathrm{m}}(\zeta_{\mathrm{m}})$ of the acceleration for optimum linear systems is $\ddot{x}_{\mathrm{m2}}^{\mathrm{LIN}}/\ddot{x}_{\mathrm{m1}} \simeq 0.25$.

4. Response of PWL System to Shock Input

In this paper, the design principle of a device with PWL asymmetric damping and linear stiffness characteristics, shown in Figure 3, is a modified version of that presented in [19], adapted for a vertical shock input.

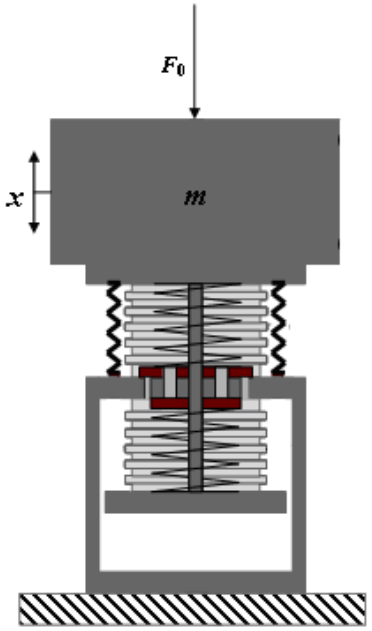

Figure 3. Design principle of a device with PWL asymmetric damping and linear stiffness characteristics.

The equation of motion for vibration isolation systems, shown in Figure 3, is given by

$$m\ddot{x} + F_{\mathrm{d}}(\dot{x}) + kx = -mV_0\delta(t),\ V_0 > 0. \tag{18}$$

where x is the absolute displacement of the sprung mass, relative to its static equilibrium position, and $F_0(t) = -mV_0\delta(t)$ is the shock applied to the sprung mass modeled by the Dirac delta function. The absolute acceleration is a measure of the mitigation of dynamic forces transmitted through the sprung mass suspension.

The asymmetrical damping characteristic is given by $F_{\mathrm{d}}(\dot{x}) = \begin{cases} c_1\dot{x}, & \dot{x} \leq 0 \\ c_2\dot{x}, & \dot{x} > 0 \end{cases}$, where $c_1, c_2 > 0$ are the damping coefficients for bound and rebound strokes, respectively, and x is the travel of the vibration isolation system.

Figures 4 and 5 show the plots of the asymmetrical damping characteristic versus velocity and displacement, respectively.

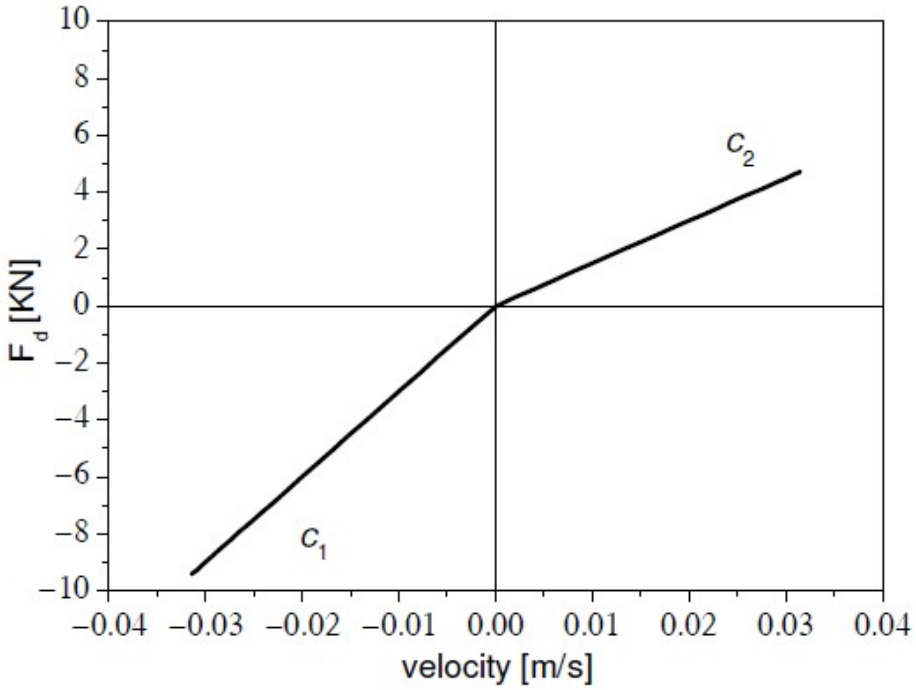

Figure 4. Asymmetric damping force versus velocity $F_{\mathrm{d}}(\dot{x})$.

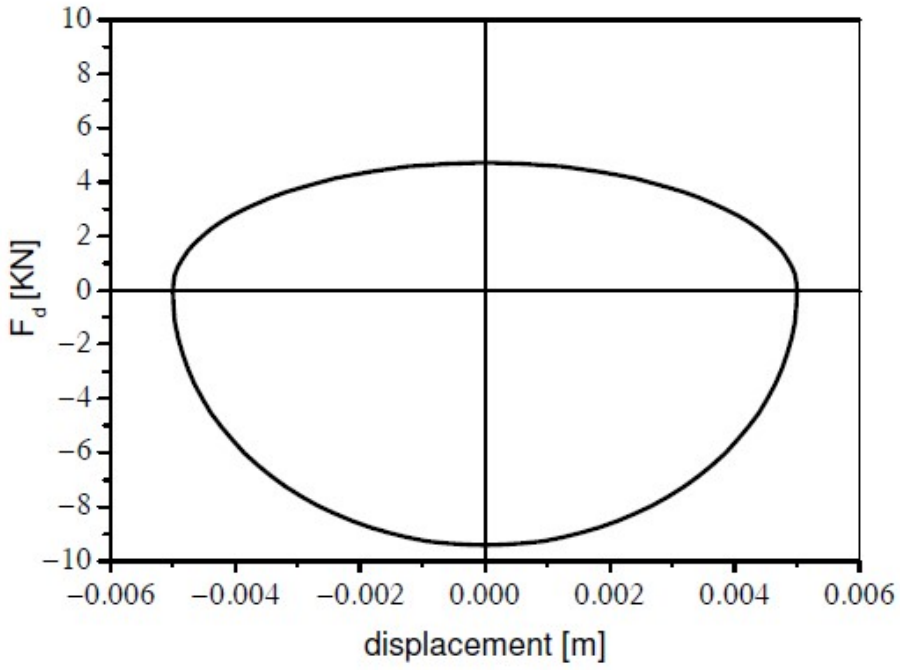

Figure 5. Asymmetric damping force versus displacement $F_{\mathrm{d}}(x)$.

The analytic expressions of asymmetric damping characteristic $F_{\mathrm{d}}(\dot{x})$, shown in Figure 4, can be written as

$$F_{\mathrm{d}}(\dot{x}) = 0.5\left[c_1(1-\mathrm{sgn}\dot{x}) + c_2(1+\mathrm{sgn}\dot{x})\right]\dot{x}. \tag{19}$$

Introducing the notations

$$\begin{array}{l} c_2 = \beta c_1,\ \omega_0 = \sqrt{\frac{k}{m}}, \\ \zeta_1 = \frac{c_1}{2\omega_0 m},\ \zeta_2 = \frac{c_2}{2\omega_0 m},\ \beta = \frac{\zeta_2}{\zeta_1}\ . \\ f_{\mathrm{d}}(\dot{x}) = \frac{F_{\mathrm{d}}(\dot{x})}{m} \end{array} \tag{20}$$

Equation (18) becomes

$$\begin{array}{l} \ddot{x} + f_{\mathrm{d}}(\dot{x}) + \omega_0^2 x = 0 \\ x(0) = 0,\ \dot{x}(0) = V_0,\ V_0 > 0 \end{array}. \tag{21}$$

where

$$f_{\mathrm{d}}(\dot{x}) = \left\{ \begin{array}{l} 2\beta\zeta_1\omega_0\dot{x},\ \dot{x} \geq 0 \\ 2\zeta_1\omega_0\dot{x},\ \dot{x} < 0 \end{array} \right. . \tag{22}$$

Relation (22) can be written as

$$f_{\mathrm{d}}(\dot{x}) = \zeta_1\omega_0\left[(\beta+1)\dot{x} + (\beta-1)\left|\dot{x}\right|\right]. \tag{23}$$

and (21) becomes

$$\left\{ \begin{array}{l} \ddot{x} + 2\zeta_2\omega_0\dot{x} + \omega_0^2 x = 0,\ \dot{x} \geq 0 \\ \ddot{x} + 2\zeta_1\omega_0\dot{x} + \omega_0^2 x = 0,\ \dot{x} < 0 \end{array} \right. . \tag{24}$$

The solution of (24) is given by

$$x(t) = \left\{ \begin{array}{l} \frac{\mathrm{V}_0}{\mathrm{A}_2} e^{-\zeta_2\omega_0 t}\sin(\mathrm{A}_2 t),\ x \in [0, \varepsilon_1] \\ \frac{\mathrm{V}_0}{A_i} e^{-\zeta_i\omega_0 t}\left[\mathrm{C}_1^{(k)}\cos(A_i t) + \mathrm{C}_2^{(k)}\sin(A_i t)\right],\ x \in [\varepsilon_k, \varepsilon_{k+1}] \end{array} \right. \tag{25}$$

where

$$i = \left\{ \begin{array}{ll} 1, & k \text{ is odd} \\ 2, & k \text{ is even} \end{array} \right. , \varepsilon_1 = \frac{1}{\mathrm{A}_2}\arctan\left(\frac{\sqrt{1-\zeta_2^2}}{\zeta_2}\right),\ \varepsilon_2 = \varepsilon_1 + \frac{\pi}{\omega\sqrt{1-\zeta_1^2}} \tag{26}$$

and

$$A_i = \omega_0\sqrt{1-\zeta_i^2},\ i = \overline{1,2},\ \varepsilon_{2k+1} = \varepsilon_1 + \frac{2k\pi}{A_2},\ k \in \mathbb{N}, \varepsilon_{2k} = \varepsilon_2 + \frac{2k\pi}{A_1},\ C_1^{(k)}, C_2^{(k)} \in \mathbb{R},\ k \in \mathbb{N}^* \tag{27}$$

For the interval $[\varepsilon_1, \varepsilon_2]$, one can derive

$$\begin{array}{l} x(\varepsilon_1) = \frac{\mathrm{V}_0}{\omega\sqrt{1-\zeta_2^2}}\mathrm{e}^{-\zeta_2\omega\varepsilon_1}\sin\left(\omega\varepsilon_1\sqrt{1-\zeta_2^2}\right) \\ x(\varepsilon_2) = \frac{\mathrm{V}_0}{A_1}e^{-\left(\frac{\pi\zeta_1}{\sqrt{1-\zeta_1^2}} + \varepsilon_1\omega\zeta_2\right)}\left\{\cos(\varepsilon_1 A_1)\left[\sin(\varepsilon_1 A_1) + \sin\left(\frac{(\pi+\varepsilon_1 A_2)A_1}{A_2}\right)\right]\zeta_1 + \right. \\ \left. + \left[-\cos(\varepsilon_1 A_1)^2 + \sin(\varepsilon_1 A_1)\sin\left(\frac{(\pi+\varepsilon_1 A_2)A_1}{A_2}\right)\right]\sqrt{1-\zeta_1^2}\right\} \\ C_1^{(1)} = \mathrm{e}^{\omega\varepsilon_1(\zeta_1-\zeta_2)}\frac{\sin\left(\omega\varepsilon_1\sqrt{1-\zeta_2^2}\right)\left[\cos\left(\omega\varepsilon_1\sqrt{1-\zeta_1^2}\right)\sqrt{1-\zeta_1^2} - \sin\left(\omega\varepsilon_1\sqrt{1-\zeta_1^2}\right)\zeta_1\right]}{\sqrt{1-\zeta_2^2}} \\ C_1^{(2)} = \mathrm{e}^{\omega\varepsilon_1(\zeta_1-\zeta_2)}\frac{\sin\left(\omega\varepsilon_1\sqrt{1-\zeta_2^2}\right)\left[\cos\left(\omega\varepsilon_1\sqrt{1-\zeta_1^2}\right)\zeta_1 + \sin\left(\omega\varepsilon_1\sqrt{1-\zeta_1^2}\right)\sqrt{1-\zeta_1^2}\right]}{\sqrt{1-\zeta_2^2}}. \end{array} \tag{28}$$

From the equation $\dddot{x}(t) = 0$, the second peak value of acceleration at the interval $[\varepsilon_1, \varepsilon_2]$ is obtained as follows:

$$\ddot{x}_{\mathrm{m2}}^{\mathrm{PWL}} = \mathrm{V}_0\omega_0\exp\left[-\left(\frac{\zeta_1\arccos\left(2\zeta_1^2-1\right)}{\sqrt{1-\zeta_1^2}} + \frac{\zeta_2\arctan\left(\frac{\sqrt{1-\zeta_2^2}}{\zeta_2}\right)}{\sqrt{1-\zeta_2^2}}\right)\right]. \tag{29}$$

The time histories of the analytic and numerical simulated displacements for $\zeta_1 = 0.25$, $\zeta_2 = 0.1$, and $f = 1$ Hz are presented in Figure 6.

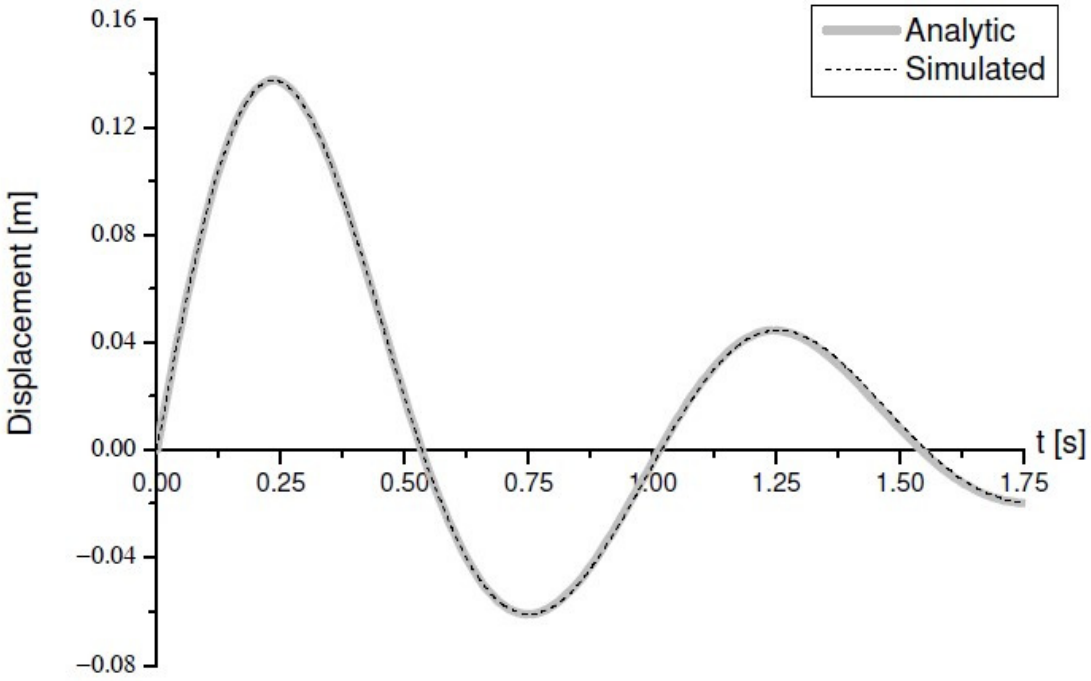

Figure 6. Time histories of analytic and simulated displacements.

5. Optimization of PWL System for Shock Input

The steps of the optimization procedure are as follows:

- For an imposed maximum feasible displacement $\overline{x}_{\mathrm{m}}$, the value of ω_{m} is determined from (16a);
- The optimum value of ζ that minimized the maximum value of absolute acceleration is $\zeta_2 = \zeta_{\mathrm{m}} = 0.4$ (for any imposed value of displacement);
- A value of ζ_1 is chosen in the interval range (0.4, 1), depending on the practical possibilities, to build shock absorbers that ensure the desired reduction in the second peak of displacement.

The beneficial effect of the asymmetry consists in the possibility of reducing the second peak of the acceleration (29) relative to the optimal linear (17), according to the graph presented in Figure 7.

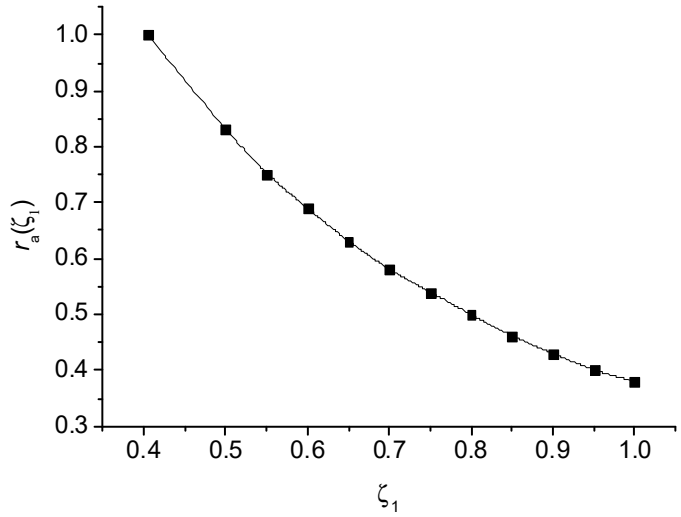

Figure 7. Ratio of second peaks of acceleration for PWL and optimum linear systems versus ζ_1.

Using this approach, the chosen solution does not lead to an increase in the maximum transmitted force, which is not possible in the linear case. Also, the output of the PWL system has fewer and smaller after-shock oscillations (better self-centering capacity) than the optimal linear system.

From relations (17) and (29), the ratio of the second peaks of acceleration for the PWL and optimum linear systems versus ζ_1, shown in Figure 7, is

$$r_a(\zeta_1) = \frac{\ddot{x}_{m2}^{PWL}(\zeta_1)}{\ddot{x}_{m2}^{LIN}(\zeta_m)}. \quad (30)$$

6. Application to Shock Isolation of Forging Hammers

In forging hammer operation, the foundations are subjected to impact loads with high intensity and short duration (shocks). In the design of these foundations, the following contradictory requirements must be taken into account:

- Maintaining the free vibration amplitudes of the equipment within the admissible limits for their stability and efficient operation. Usually, the maximum displacement x_m should be less than 0.006 m.
- Reducing as much as possible the transmissibility of the dynamic loads produced by the operation of the forging hammer to the foundation structure.
- Ensuring the proper frequency of the free oscillations produced by the impact of the hammer, which is approx. 2 times higher than that corresponding to the maximum number of strokes per minute that the machine can produce (approx. 200 strokes/min, i.e., approx. 3.3 Hz).

In general, to achieve these goals, devices with elastic and dissipative properties are used for the base isolation of a forging hammer [16,20]. In this paper, we considered the case study of a forging hammer (Figure 8) with the following characteristics:

- Hammer weight: 1250 kg;
- Assembly weight: 36,000 kg;
- Maximum shock energy: 36 kJ.

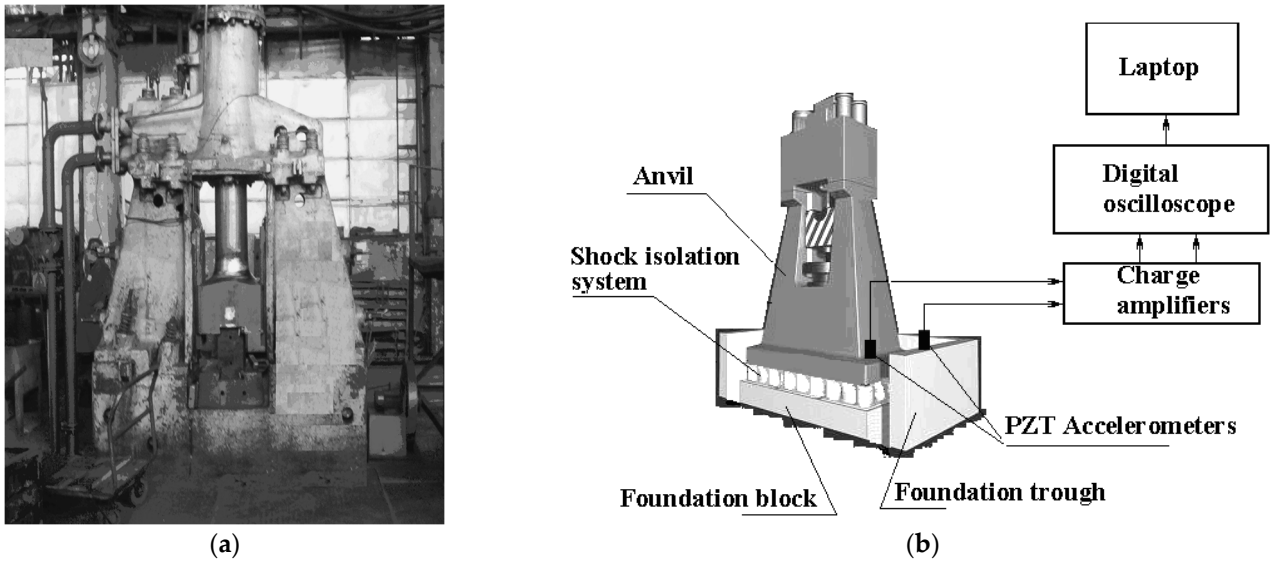

Figure 8. Forging hammer system: (**a**) in situ, (**b**) schematic.

The shock isolation system consists of linear springs and viscous damping modules. In Figure 9, schematics of the shock isolation device (left) and the design principle (right) are presented.

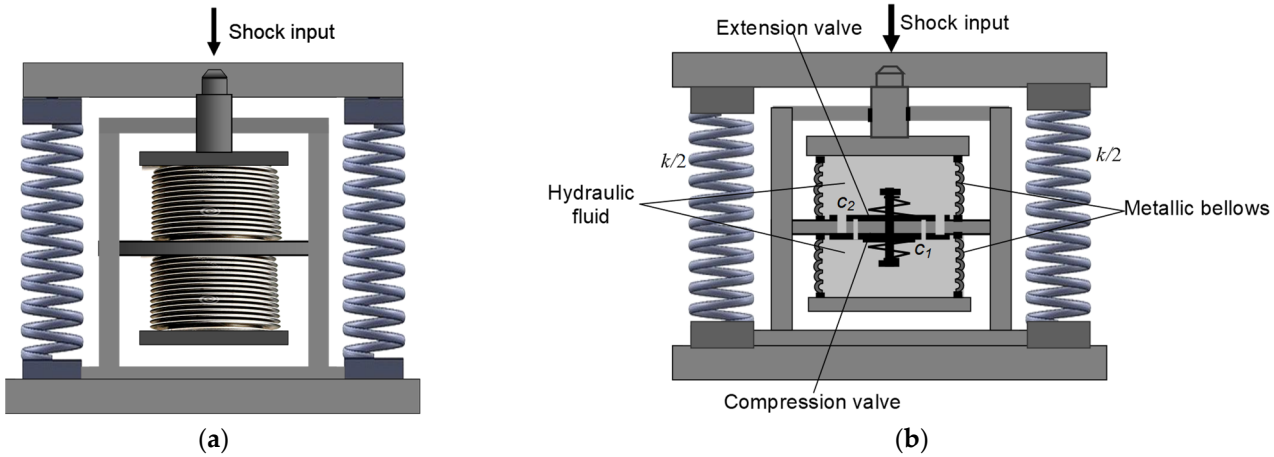

Figure 9. Schematics of (**a**) linear springs and (**b**) viscous damping module.

The metallic bellows, filled with hydraulic fluid, are welded at both ends and, therefore, the fluid damper is leak-proof. The asymmetry of the damping force shown in Figure 5 is controlled by the openings of compression and extension valves ($c_1 > c_2$). The dimensions of the valve openings and fluid viscosity must be assessed so as to have laminar flow within the range of damper operating conditions. Since the bellows geometry is identical, there is no need for any volume compensation system.

Figure 10 shows a sequence of hammer strikes recorded on the anvil block under operating conditions. Since the recorded shock accelerations are significantly affected by the structural noise, in order to compare the efficiency of the proposed PWL system, a linear system is identified based on the shock response. The parameters of the linear SDOF model (2), identified from experimental data, are $f = 7.3$ Hz, $\zeta = 0.12$, $V_0 = 0.43$ m/s. The output of this system is plotted in Figure 11.

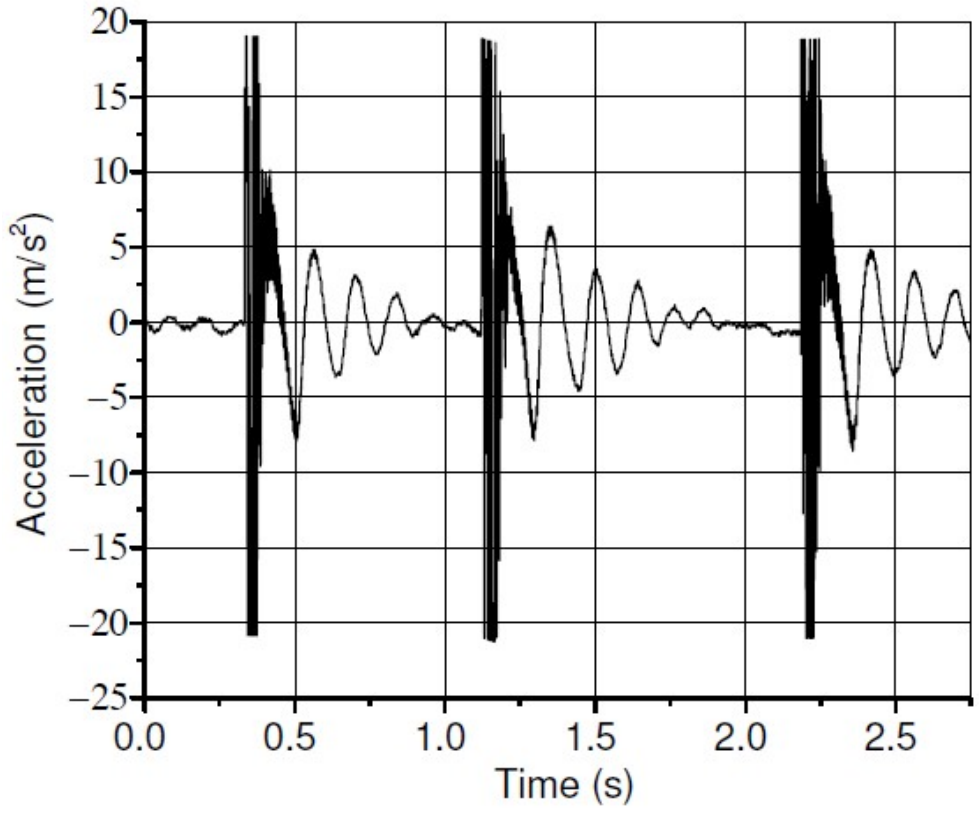

Figure 10. The recorded time history of three consecutive strikes.

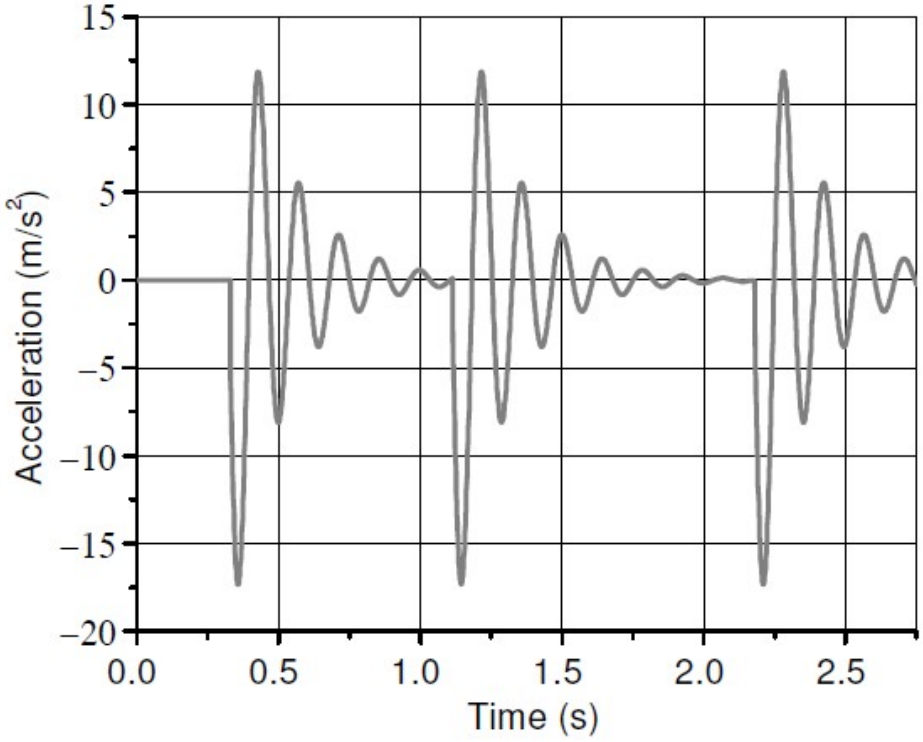

Figure 11. Calculated output of identified linear systems for three consecutive strikes.

The amplitude spectra of the measured and calculated acceleration responses determined by applying FFT for the after-shock records corresponding to one strike are shown in Figure 12.

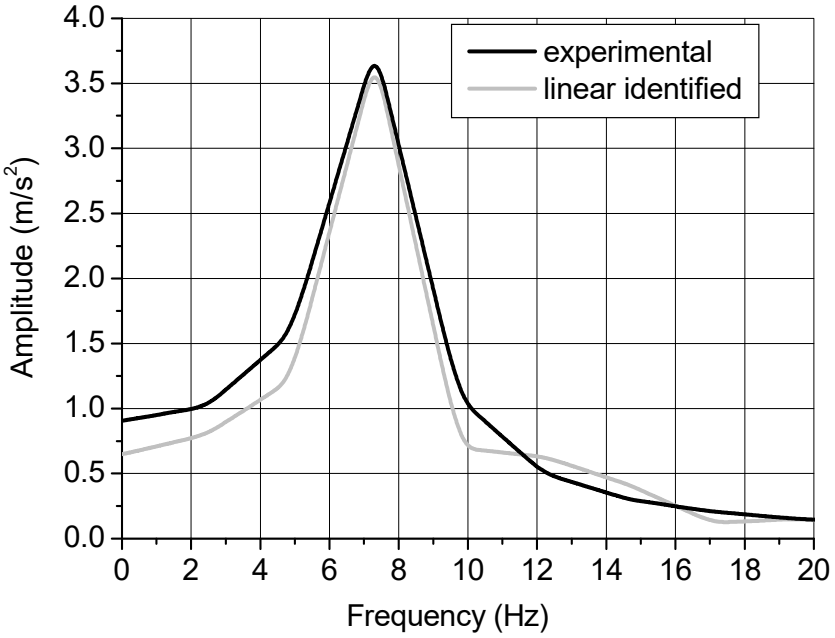

Figure 12. Amplitude spectra of measured and calculated acceleration responses.

The calculated acceleration and displacement for the identified linear, linear optimum, and PWL systems are shown in Figures 13 and 14. As one can see, the after-shock oscillations are significantly reduced in the case of the PWL system.

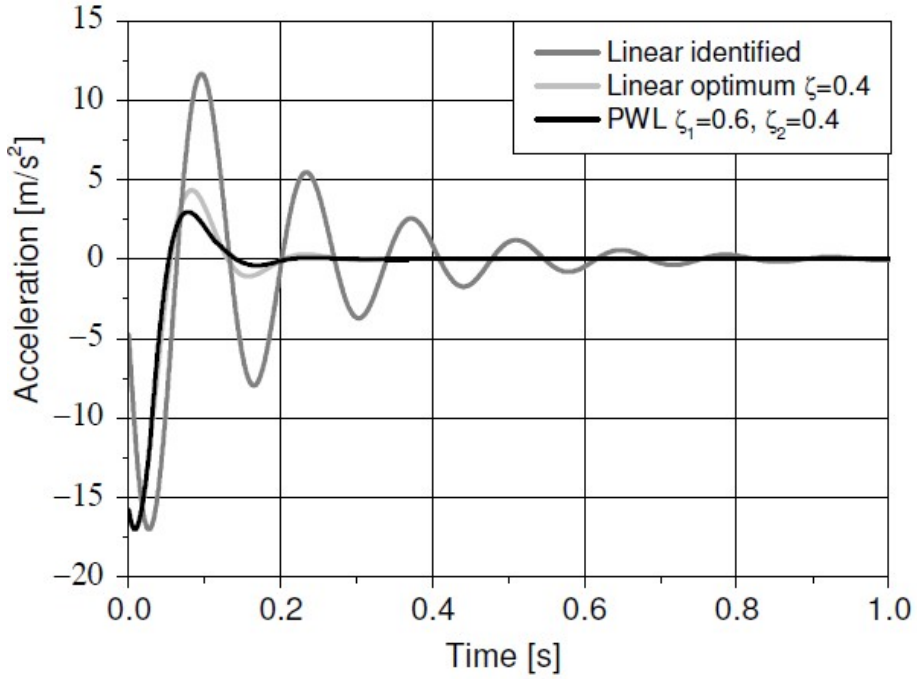

Figure 13. Calculated accelerations for identified linear, linear optimum, and PWL systems.

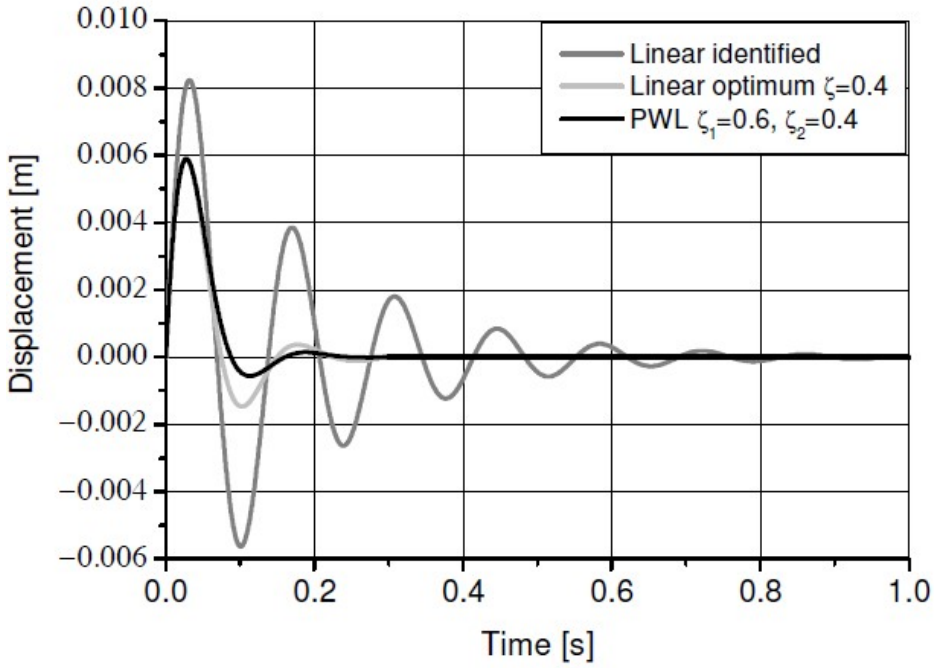

Figure 14. Calculated displacements for identified linear, linear optimum, and PWL systems.

7. Conclusions

The output of an SDOF piecewise linear system with asymmetric damping and linear stiffness, excited via Dirac impulse excitation, is analytically determined. Using the analytical results, an optimization procedure of a PWL system for shock input is proposed for the damping optimization of a shock isolation system.

By using PWL shock isolation systems, optimized according to the proposed procedure described in this paper, one can obtain better fulfillment of the following requirements: minimum absolute acceleration, maximum imposed displacement, and a substantial reduction in after-shock vibrations. This improvement leads to the possibility of shortening the action time of the forging hammer between two blows.

Author Contributions: All four authors conceived the framework and structured the whole manuscript, checked the results, and completed the revision of the paper. The authors equally contributed to the elaboration of this manuscript. All authors have read and agreed to the published version of the manuscript.

Funding: This research received no external funding.

Data Availability Statement: The data of this study are available from the corresponding authors upon reasonable request.

Conflicts of Interest: The authors declare no conflict of interest.

References

1. Hundal, M.S. Response of shock isolators with linear and quadratic damping. *J. Sound Vib.* **1981**, *76*, 273–281. [CrossRef]
2. Lou, J.; Sun, J.; Tang, S.; Li, H. Study on the optimization of the shock isolation system based on the limiting performance analysis. *Int. J. Dyn. Control* **2014**, *2*, 415–424. [CrossRef]
3. Yadav, S.; Yap, F.F.; Peh, T.S. Design and Analysis of Shock Isolators. In Proceedings of the 20th Hwarangdae International Symposium: The 7th International Conference on Design and Analysis of Protective Structures, Seoul, Republic of Korea, 4–6 December 2019.
4. Balike, K.P.; Rakheja, S.; Stiharu, I. Influence of suspension kinematics and damper asymmetry on the dynamic responses of a vehicle under bump and pothole excitations. *SAE Tech. Pap.* **2010**, *54*, 191–216.
5. Chicurel-Uziel, E. Exact, single equation, closed-form solution of vibrating systems with piecewise linear springs. *J. Sound Vib.* **2001**, *245*, 285–301. [CrossRef]
6. Sireteanu, T.; Mitu, A.M.; Niculescu, A.I.; Kowalski, M.; Jankowski, A. Condition monitoring of vehicle dampers using shock excitation. *Proc. Rom. Acad. Ser. A Math. Phys. Tech. Sci. Inf. Sci.* **2019**, *20*, 87–95.
7. Zhao, L.L.; Yang, F.X.; Yu, Y.W.; Zhou, C.C.; Mao, S.F. Influence of shock absorber asymmetry on vibration responses of seat-occupant system under impact condition. In Proceedings of the 9th International Conference on Modelling, Identification and Control (ICMIC), Kunming, China, 10–12 July 2017; pp. 394–399. [CrossRef]
8. Vaiana, N.; Marmo, F.; Sessa, S.; Rosati, L. Modeling of the Hysteretic Behavior of Wire Rope Isolators Using a Novel Rate-Independent Model. In *Nonlinear Dynamics of Structures, Systems and Devices*; Lacarbonara, W., Balachandran, B., Ma, J., Tenreiro Machado, J., Stepan, G., Eds.; Springer: Cham, Switzerland, 2020. [CrossRef]
9. Pellecchia, D.; Vaiana, N.; Spizzuoco, M.; Serino, G.; Rosati, L. Axial hysteretic behaviour of wire rope isolators: Experiments and modelling. *Mater. Des.* **2023**, *225*, 111436. [CrossRef]
10. Ruzicka, J.E. Passive shock isolation. Part I. *J. Sound Vib.* **1970**, *4*, 1–11.
11. Ruzicka, J.E. Passive shock isolation. Part II. *J. Sound Vib.* **1970**, *4*, 12–24.
12. Suhir, E. Dynamic response of a one-degree-of-freedom linear system to a shock load during drop tests: Effect of viscous damping. *IEEE Trans. Compon. Packag. Manuf. Part A* **1996**, *19*, 435–440. [CrossRef]
13. Dinca, F.; Teodosiu, C. *Nonlinear and Random Vibration*; Academic Press: New York, NY, USA, 1973.
14. El Hifnawy, L.; Novak, M. Response of hammer foundations to pulse loading. *Soil Dyn. Earthq. Eng.* **1984**, *3*, 124–132. [CrossRef]
15. Ghafar Chehab, A.; Hesham El Naggar, M. Response of block foundations to impact loads. *J. Sound Vib.* **2004**, *276*, 293–310. [CrossRef]
16. Wang, G.; Dong, Z. Design optimization of low impact transmission foundation for forging hammers. *Eng. Comput.* **2006**, *23*, 166–186. [CrossRef]
17. Trabka, A. Effect of Pulse Shape and Duration on Dynamic Response of a Forging System. *Acta Mech.* **2019**, *13*, 226–232. [CrossRef]
18. Saberi, S.; Fischer, J.; Stockinger, M.; Tikal, R.; Afsharnia, R. Theoretical and experimental investigations of mechanical vibrations of hot hammer forging. *Int. J. Adv. Manuf. Technol.* **2021**, *114*, 3037–3045. [CrossRef]
19. Sireteanu, T.; Mitu, A.-M.; Solomon, O.; Giuclea, M. Approximation of the Statistical Characteristics of Piecewise Linear Systems with Asymmetric Damping and Stiffness under Stationary Random Excitation. *Mathematics* **2022**, *10*, 4275. [CrossRef]
20. Mitu, A.M.; Sireteanu, T.; Baldovin, D.C. Design of a new base isolation system for forging hammer. In Proceedings of the 9th WSEAS International Conference on Acoustics & Music: Theory & Applications, Bucharest, Romania, 24–26 June 2008; pp. 77–82.